
DOMAIN GENERALISATION FOR OBJECT DETECTION *

Karthik Seemakurthy, Petra Bosilj

Lincoln Institute of Agri-Food Technology
University of Lincoln
Lincoln, UK

{kseemakurthy, pbosilj}@lincoln.ac.uk

Charles Fox

School of Computer Science
University of Lincoln
Lincoln, UK

chfox@lincoln.ac.uk

Erchan Aptoula

Institute of Information Technologies
Gebze Technical University
Gebze, Kocaeli, Turkey
eaptoula@gtu.edu.tr

ABSTRACT

Domain generalisation aims to promote the learning of domain-invariant features while suppressing domain specific features, so that a model can generalise well on previously unseen target domains. This paper studies domain generalisation in the object detection setting. We propose new terms for handling both the bounding box detector and domain belonging, and incorporate them with consistency regularisation. This allows us to learn a domain agnostic feature representation for object detection, applicable to the problem of domain generalisation. The proposed approach is evaluated using four standard object detection datasets with available domain metadata, namely GWHD, Cityscapes, BDD100K, Sim10K and exhibits consistently superior generalisation performance over baselines.

Keywords Domain Generalisation · Object Detection · Domain Invariance

1 Introduction

Object detection is the task of identifying and localising all instances of a certain object in an image. Benchmark performances have increased significantly using deep learning approaches [1, 2, 3, 4, 5, 6, 7, 8]. Factors such as viewpoint, background, weather, and image quality increase the variations in object appearance (examples from autonomous farming and driving in Fig. 1). The resulting distribution discrepancy between training and testing data is called *domain shift* and degrades model performance at deployment [9, 10].

Although increasing the amount and diversity of training data can alleviate the impact of domain shift in theory, image annotation remains an expensive and time consuming task, and there can be no guarantee that all deployment scenarios will be adequately represented. *Domain adaptation* (DA) [11, 12, 13, 14, 15, 16] addresses domain shift by adapting the parameters of the trained model by exploiting unlabelled data from the target domain(s). However, in practice target domain data is often sparse and unavailable.

In contrast to DA, *domain generalisation* (DG) aims to learn a single, unchanging set of parameters which are able to perform well on previously unseen domains. It achieves this by training on several domains and ensuring that the domain-specific information is suppressed. It is a harder yet more valuable setting than DA as it requires no data from the target domain, nor a separate adaptation step [17]. However, recent surveys on this topic [18, 19] show that very little work has been done on DG for object detection [20]. This is the first systematic study of DG for object detection, where domain shift for object detection has so far been mainly studied for DA.

**Citation:* Authors. Title. Pages.... DOI:000000/11111.

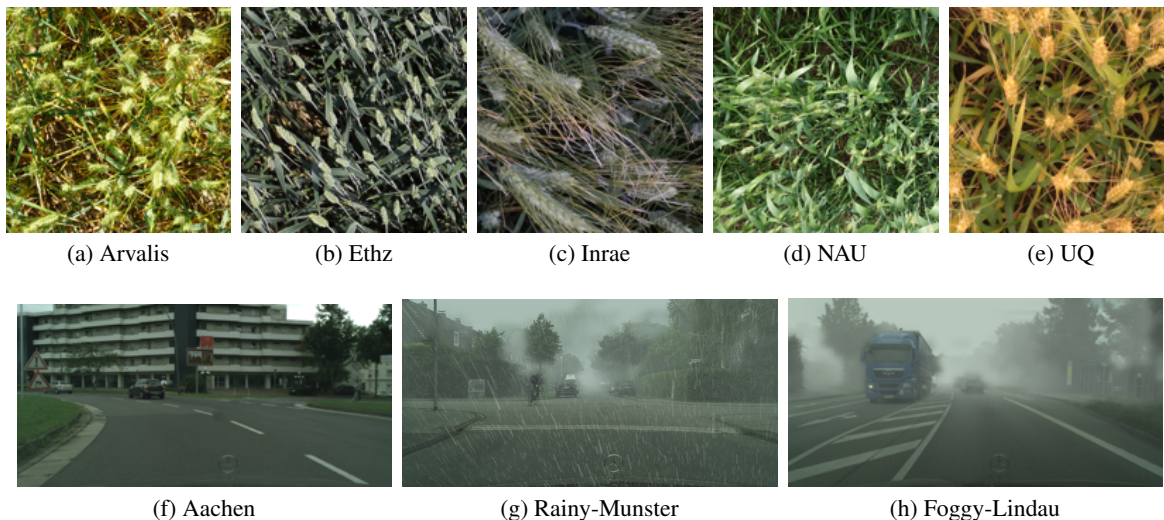


Figure 1: Samples from various training and testing domains in the Global Wheat Head Detection (GWHD) (a)-(e) and Cityscapes (f)-(h) datasets used in our experiments.

Furthermore, this is the first paper to address domain shift for object detection without assuming the covariate shift case. While the assumption that the conditional distributions are approximately equal was disputed and addressed in classification [21], techniques which improve classification do not always directly translate to improvements on more complex tasks such as object detection. We offer a rigorous mathematical analysis of domain shift, without assuming equality of the conditionals, specifically for the object detection setting. Inspired by [21], we propose a new bounding box loss which, together with a consistency regularisation method previously used in DA [11], allows us to perform end-to-end training of an object detection model².

Experimental validation has been conducted on four datasets: Sim10K [22], Cityscapes [23], BDD100K [24], and GWHD [25]. We evaluate a multi-object detection scenario on a single target domain for autonomous driving, and a single-object detection scenario with multiple target domains for autonomous agriculture. Among a number of established and newly proposed DG benchmarks and datasets [26, 19, 18, 27, 28], object detection is explicitly addressed **only** on GWHD. Experiments on Cityscapes have been designed to retain similarities with the typical DA setting and facilitate a comparison between the two approaches for addressing domain shift. The experimental results demonstrate the effectiveness of the proposed DG approach in all the scenarios. We use Faster R-CNN [4] as a baseline detection for validation purposes, however the proposed theory is applicable to any other parametric feature based object detection model.

2 Related Work

The proposed system builds upon work in object detection, domain adaptation and domain generalisation.

Object detection. Classical approaches to object detection relied on handcrafted features and formulated object detection as a sliding window classification problem [29, 30, 31]. The empirical success of convolutional neural networks (CNNs) – which automatically extract high performing features – [32, 33] has resulted in their widespread adoption. Most CNN-based approaches to object detection can be categorised as either single-stage [34, 1, 2, 3] or two-stage [35, 36, 4, 5, 6]. Single-stage approaches perform localisation and classification simultaneously and have only recently reached the performance of two-stage approaches [1]. Two-stage approaches developed from the Region-based CNN (R-CNN) family on the other hand [35, 36, 4], are characterised by a network trained to classify region proposals selected from the image. Region proposals were initially selected by a static shallow approach and processed independently [35]. R-CNN was then extended to use a shared feature map for all the region proposals from the same image [36]. Faster R-CNN additionally [4] introduced a Region Proposal Network (RPN), producing object proposals as well as the feature maps used for region classification, thus resulting in an end-to-end trainable system. However, all of these architectures and a number of follow-up works [3, 6, 5] operate under the assumption that the

²code will be published upon paper acceptance

testing data originates from the same domain and distribution as the training data and their performance consequently degrades on out-of-domain (OOD) data.

Domain adaptation. Chen *et al.* [11] proposed a domain adaptation approach for the object detection problem where they align the image- and instance-level domain classifiers via a consistency regulariser. In fact, they assume that the instance level classifier is consistent across domains, which however is false, when there is a significant shift in the input image domains [21, 37, 38, 39]. Subsequent attempts of DA for object detection [15, 40] include using adversarial learning to diminish domain discrepancy [11, 41, 13, 14, 42, 43], reconstruction-based methods using image style transfer as an auxiliary task [16, 44, 45], and self-training methods using pseudolabels to retrain a model [46, 47]. Furthermore, the aforementioned approaches consider a single source and target domain, with multi-source DA for object detection having been considered only recently [48].

One of the latest studies [12] on this topic employs an uncertainty-aware model, where a Bayesian CNN based framework obtains an uncertainty estimate from the classification and regression sub-networks of a detector. This estimate is used for selecting the pseudo-labels generated from the target domain samples, which in turn are exploited for augmenting the training data.

The present study is most closely related to adversarial approaches which align feature representations of source and target domains, although in our case we align features from multiple source domains. More specifically, we build upon Chen *et al.* [11], by not only deploying it in the multi-source DG setting, but also by extending it with regulariser terms, which align the feature distributions stemming from various source domains.

Domain generalisation. DG was first studied by Blanchard *et al.* [49] in the context of medical imaging, while the terminology was introduced later by Muandet *et al.* [50]. Earlier studies have explored fixed shallow features [26, 51, 52, 50, 53], while more recent investigations design architectures to address domain shift [17] or learning algorithms to optimise standard architectures [54, 55, 56]. Domain randomisation [57, 58] is a complementary approach to DG, which relies on synthetically generated variations of the input data to obtain more generalisable features.

A drawback of many of the earlier approaches to DG, addressed explicitly in this paper, is the assumption that the conditional class distribution does not vary across source domains. This has recently been identified and addressed in the classification setting [21, 37, 59, 60]. In this paper, we adopt the domain generalised entropy based regularisation (DG-ER) approach proposed by Zhao *et al.* [21] for the object detection problem to achieve class conditional invariance and we also show that consistency based regularisation can help us achieve invariant bounding box regression across domains.

As shown by the recent surveys of the area, the vast majority of work on DG has been conducted in the classification setting [19, 18]. Domain randomisation was applied to car detection [61], however their approach requires 3D models of the detected objects to generate the synthetic data, and assumes knowledge of the camera parameters and the scene geometry. A single-shot YOLO detector has also been extended with DG components [62, 20], which differs from our work as they use Invariant Risk Minimisation (IRM) [63] to achieve consistent detection across domains. However, IRM is likely to underperform when there is a significant domain shift [64]. This renders it unsuitable for scenarios exhibiting a very high visual cross-domain diversity, such as wheat head detection (Fig. 1).

3 Preliminaries

In this section we describe the details of the mathematical framework used to describe the DG task for object detection. This framework is then used to present the proposed method in the following Section.

We define a *parametric feature based detector (model)* to be any function which takes an image as input, transforms it to some vector of features according to parameters, and returns a set of bounding boxes and for each bounding box, a vector of class probabilities based only on these features and additional parameters. We further define a *trainer* as any system which takes images, ground truth bounding boxes and object classes of these bounding boxes, and a loss function, all as input; and returns a set of parameters which minimises the loss function between the model outputs and the training data, called a *trained model*. Faster-RCNN is the paradigm case, but many other detection systems share this structure, on which the new method can operate.

DG assumes that the training data is generated from N domains. The goal is to build a trainer that can learn domain-invariant features from these N source domains which can be generalised to an unseen target domain (or domains) without compromising the classification and bounding box prediction performance.

Let $\mathbf{I} \times \mathbf{C} \times \mathbf{B} \times \mathbf{D}$ be the sample space under observation. Here $I \in \mathbf{I}$ denotes the images of interest. $B^I \in \mathbb{R}^4 = \mathbf{B}$ is the bounding box predictor consisting of a vector of image coordinates (x, y, w, h) corresponding to the objects detected in image I . $C^I \in \{0, \dots, K\} = \mathbf{C}$ denotes the integer-valued class label assigned to each of the detected

bounding boxes B^I , where K is the total number of object classes, and $D^I \in \mathbf{D}$ represents the domain of image I . Let $P_D(I, C^I, B^I)$ denote the joint distributions defined on the sample space $\mathbf{I} \times \mathbf{C} \times \mathbf{B}$ given domain D . The proposed method takes as input a model, a trainer, and data from $\mathbf{I} \times \mathbf{C} \times \mathbf{B} \times \mathbf{D}$. It returns a trained model which provides domain invariant detection. This is accomplished via a novel loss function which promotes DG and is passed to the trainer.

Let (θ, ϕ, β) be the parameters for a feature extractor $F^{(\theta)}$, a classifier $T^{(\phi)}$, and a bounding box predictor $R^{(\beta)}$, respectively. Let $Q^{T^{(\phi)}, R^{(\beta)}}(F^{(\theta)}(I), C^I, B^I)$ be the model joint distribution obtained when using all of these parameters together. The goal of the work is to optimise θ to transform the input images into feature vectors $F^{(\theta)}(I)$ such that all the domain specific joint distributions $P_D(F^{(\theta)}(I), C^I, B^I)$ converge to the single best (maximising the fit over ϕ and β) joint distribution $Q^{T^{(\phi)}, R^{(\beta)}}(F^{(\theta)}(I), C^I, B^I)$. This will enable $F^{(\theta)}$, $T^{(\phi)}$ and $R^{(\beta)}$ to be optimised for domain invariant object detection. According to Bayes' theorem, in order to map the domain specific joint distributions $P_D(F^{(\theta)}(I), C^I, B^I)$ to a common $Q^{T^{(\phi)}, R^{(\beta)}}(F^{(\theta)}(I), C^I, B^I)$, we need to map the domain specific conditionals $P_D(C^I, B^I | F^{(\theta)}(I))$ to a common $Q^{T^{(\phi)}, R^{(\beta)}}(C^I, B^I | F^{(\theta)}(I))$ and the domain specific marginals $P_D(F^{(\theta)})$ need to be mapped onto a common $Q(F^{(\theta)})$.

In fact, many of the reported studies in the state-of-the-art [11, 50] attribute domain shift to the difference in marginals, while they assume conditionals to be stable across domains. The standard approach adopted by [11, 65] of equalising the marginals across domains is through an explicit domain discriminator $S^{(\psi)}$, which is trained by minimising the following negative discriminator ('domain adversarial' or 'dadv') loss [66],

$$\min_{\theta} \max_{\psi} L_{dadv}(\theta, \psi) = \sum_{D=1}^N \mathbb{E}_{P_D} \left[\log \left(S^{(\psi)} \left(F^{(\theta)}(I) \right) \right) \right] = \sum_{D=1}^N \sum_{j=1}^{M_D} \mathbf{d}_j^D \cdot \log \left(S^{(\psi)} \left(F^{(\theta)}(I_j^D) \right) \right) \quad (1)$$

where \mathbf{d}_j is the one-hot vector encoding of the domain label of the j -th image sample, and M_D is the number of samples in the D -th domain. The maximisation is conducted with respect to parameters corresponding to the domain discriminator $S^{(\psi)}$, while the minimisation is with respect to the feature extractor $F^{(\theta)}$. This minmax game enables $F^{(\theta)}$ to learn features whose domain cannot be distinguished by any $S^{(\psi)}$. This implies that the optimisation in Eq. (1) will lead to equality in marginals,

$$\begin{aligned} P_i(F^{(\theta)}(I)) &= P_j(F^{(\theta)}(I)), \forall i, j \in \{1, \dots, N\} \\ &= Q(F^{(\theta)}(I)) \end{aligned} \quad (2)$$

However, as pointed out by recent studies [38, 39, 37, 21], the stability of conditionals across domains cannot be guaranteed. Any method with the goal of achieving domain invariance needs to compensate for the variation in conditionals $P_D(C^I, B^I | F^{(\theta)}(I))$. In other words, the domain discriminator $S^{(\psi)}$ aids in achieving the invariance on the sample space $\mathbf{I} \times \mathbf{D}$ but not on $\mathbf{I} \times \mathbf{C} \times \mathbf{B} \times \mathbf{D}$. Moreover, the techniques proposed in recent studies [21, 37] are intended for classification and cannot be directly used to achieve generalised object detection.

In the next section, we describe the details of the proposed mathematical framework, to map the domain-specific conditionals $P_D(C^I, B^I | F^{(\theta)}(I))$ to a common $Q^{T^{(\phi)}, R^{(\beta)}}(C^I, B^I | F^{(\theta)}(I))$. Our approach in conjunction with Eq. (1) will lead to domain generalised object detection.

4 Proposed Method

The block diagram of the proposed approach is given in Fig. 2. It assumes that a parametric feature based detector model is provided which includes (by our definition) separable feature extraction and detection modules; such as, but not limited to, Faster R-CNN. It adds two further modules related to class-conditional invariance and bounding box invariance, which aid to optimise the feature extractor, in order to map the input images into feature vectors so that the detection is consistent across multiple domains. In this section, we elaborate on these new modules.

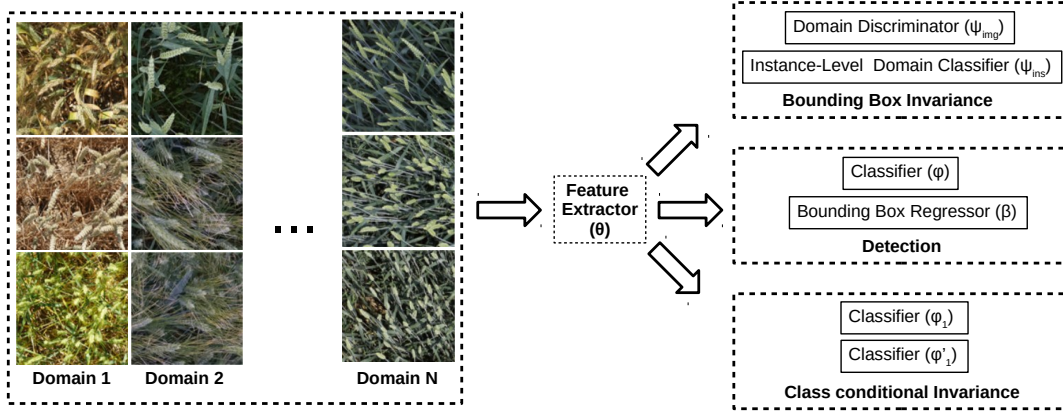


Figure 2: Block diagram of the proposed approach.

We aim to transform the domain-specific conditional distribution in every D -th domain to a common distribution $Q^{T(\phi), R(\beta)}(C^I, B^I | F^\theta(I))$. This can be done by minimising the KL divergence between all of the P_D and $Q^{T(\phi), R(\beta)}$:

$$\begin{aligned} & \min_{\theta, \phi, \beta} \sum_{D=1}^N KL[P_D(C^I, B^I | F^\theta(I)) || Q^{T(\phi), R(\beta)}(C^I, B^I | F^\theta(I))] \\ & = \min_{\theta, \phi, \beta} \sum_{D=1}^N KL[P_D(C^I | B^I, F^\theta(I)) || Q^{T(\phi)}(C^I | B^I, F^\theta(I))] \\ & \quad + \sum_{D=1}^N KL[P_D(B^I | F^\theta(I)) || Q^{R(\beta)}(B^I | F^\theta(I))] \end{aligned} \quad (3)$$

where $Q^{T(\phi)}(C^I | B^I, F^\theta(I))$ and $Q^{R(\beta)}(B^I | F^\theta(I))$ denote respectively the distributions associated with the instance level classifier and the bounding box predictor. The minimisation of the first term in Eq. (3) trains the system to transform the input images into a feature space where the domain-specific instance level classifier will be consistent across the domains. The minimisation of the second term in Eq. (3) trains the system to transform input images into a feature space where the bounding box predictor is invariant to any individual domain. This implies that the optimisation in Eq. (3) along with Eq. (1) will result in a domain generalised trained model.

The first term in Eq. (3) can be further modified as:

$$\sum_{D=1}^N \mathbb{E}_{P_D} \left[\log \frac{P_D(C^I | B^I, F^\theta(I))}{Q^{T(\phi)}(C^I | B^I, F^\theta(I))} \right] = \sum_{D=1}^N \mathbb{E}_{P_D} \left[\log P_D(C^I | B^I, F^\theta(I)) \right] - \sum_{D=1}^N \mathbb{E}_{P_D} \left[\log Q^{T(\phi)}(C^I | B^I, F^\theta(I)) \right] \quad (4)$$

The second term in Eq. (4) denotes the classification loss L_{cls} , while the first term is the sum of N negative conditional entropies $-H_D(C^I | B^I, F^\theta(I))$ for each domain. Minimising the negative conditional entropy is equivalent to maximising the conditional entropy $H_D(C^I | B^I, F^\theta(I))$. This implies that maximising the conditional entropy $H_D(C^I | B^I, F^\theta(I))$ for a specific domain D can increase the uncertainty in assigning the correct class label for the objects in the input image I . In order to maximise the conditional entropy $H_D(C^I | B^I, F^\theta(I))$ in Eq. (4), we adopt the following theorem from [21] for object detection:

Theorem 1: Assuming all the object classes are equally likely, maximising $H_D(C^I | B^I, F^\theta(I))$ is equivalent to minimising the Jensen-Shannon divergence between the conditional distributions $P_D(B^I, F^\theta(I) | C = j)_{j=1}^K$. The global minimum can be achieved if and only if:

$$\begin{aligned} P_D(B^I, F^\theta(I) | C^I = i) &= P_D(B^I, F^\theta(I) | C^I = j), \\ &\forall i, j \in \{1, \dots, K\}. \end{aligned} \quad (5)$$

Even though this assumption can fail under a class imbalance scenario, balance can still be enforced through batch based biased sampling. The detailed proof is given in Appendix A.

The intuition behind Eq. (20) is that the minimisation of class conditional entropy results in domain specific instance level features which do not have the discriminative ability to assign the correct class label corresponding to the objects in the image I . As mentioned in the main paper, we realise the result in Eq. (20) by introducing the additional N domain specific classifiers. Also, following [21], we use gradient reversal layer (GRL) to aid the feature extractor lose the discriminative ability while minimising the domain specific classification loss.

The equality in conditionals $P_D(B, F_\theta(I)|C = j)$ for all the classes implies that the instance level features extracted are independent of the class labels. Inspired by Theorem 1 and the minmax game approach proposed in [66, 67, 21], we introduce N classifiers, $\{T_D^{(\phi'_D)}\}_{D=1\dots N}$, each parameterised by a ϕ'_D , and propose the following loss function,

$$\min_{\theta} \max_{\{\phi'_D\}_{D=1}^N} L_{erc}(\theta, \phi'_i) = \sum_{D=1}^N \mathbb{E}_{P_D} \left[\log Q_D^{T_D^{(\phi'_D)}}(C|B, F^{(\theta)}(I)) \right], \quad (6)$$

where $Q_D^{T_D^{(\phi'_D)}}(C|B, F^{(\theta)}(I))$ is the instance-level class conditional probability induced by classifier T_D corresponding to the D -th domain.

To optimise the second term in Eq. (3), we adopt a strategy previously used by [11] for DA. Minimising the KL divergence between the terms $P_D(B|F^{(\theta)}(I))$ and $Q^{R^{(\beta)}}(B|F^{(\theta)}(I))$ is equivalent to building a bounding box predictor independent of the domain label D . Rewriting the term $P_D(B|F^{(\theta)}(I))$ as $P(B|D, F^{(\theta)}(I))$, and using Bayes' theorem, gives:

$$P(D|B, F^{(\theta)}(I))P(B|F^{(\theta)}(I)) = P(B|F^{(\theta)}(I), D)P(D|F^{(\theta)}(I)), \quad (7)$$

where $P(D|B, F^{(\theta)}(I))$ represents the instance level domain label predictor, $P(B|F^{(\theta)}(I), D)$ is the domain specific bounding box predictor, and $P(D|F^{(\theta)}(I))$ is the image level domain label predictor. From Eq. (1), we can observe that if there is a consistency between the image and instance level domain label predictor then the bounding box predictor will be invariant to domains, i.e. $P(B|D, F^{(\theta)}(I)) = P(B|F^{(\theta)}(I))$.

The input $F^{(\theta)}(I[B])$ to the instance-level domain classifier will be the subset of image I features, computed at locations within the bounding box B by $F^{(\theta)}$. The loss function that is employed at the instance level domain classifier is:

$$L_{Dins} = \sum_{|B|} \mathbb{E} \left[\log(P(D|B, F^{(\theta)}(I))) \right], \quad (8)$$

where $|B|$ denotes the total number of detected bounding boxes in the image I . As shown in Eq. (7), in order to achieve invariant bounding box prediction across domains, we need a consistency regularisation [11]:

$$L_{cst} = \left\| \frac{1}{|B|} \sum_{i=1}^{|B|} (\mathbf{p}_i^{ins} - \mathbf{p}^{img}) \right\|_2, \quad (9)$$

where \mathbf{p}_i^{ins} and \mathbf{p}^{img} denote respectively the probability scores corresponding to the instance and domain level classifier outputs.

The main loss function that is to be used for training the system is given by:

$$\begin{aligned} \min_{(\theta, \phi)} \max_{(\psi_{img}, \{\phi'_D\}, \psi_{ins})} & L(\theta, \phi, \psi_{img}, \psi_{ins}, \{\phi'_D\}, \beta) \\ & = L_{cls}(\theta, \phi) + L_{reg}(\theta, \beta) \\ & + \alpha_1 L_{dadv}(\theta, \psi_{img}) + \alpha_2 L_{dins}(\theta, \psi_{ins}) \\ & + \alpha_3 L_{cst}(\theta, \beta) + \alpha_4 L_{erc}(\theta, \{\phi'_D\}), \end{aligned} \quad (10)$$

where $\alpha_1, \alpha_2, \alpha_3, \alpha_4$ represent the regularisation constants.

It is important to note that the features learned via the maximisation of the domain specific classification loss L_{erc} can have a negative impact on the classifier $T^{(\phi)}$, and on the bounding box predictor $R^{(\beta)}$, and thus can result in instability during the mini-max optimisation of Eq. (10). To overcome this drawback, following [21], we introduce N additional

domain-specific classifiers, $\{T_D^{\dagger(\phi_D^\dagger)}\}_{D=1}^N$, with a new cross-entropy loss:

$$\begin{aligned} \min_{\theta, \{\phi_D^\dagger\}_{D=1}^N} L_{cel}(\theta, \{\phi_D^\dagger\}_{D=1}^N) = & - \sum_{D=1}^N \mathbb{E}_{P_D} [\log Q_{T_D^{\dagger(\phi_D^\dagger)}}(C|B, \bar{F}(I))] \\ & - \sum_{D=1}^N \sum_{j=1, j \neq D}^N \mathbb{E}_{P_j} [\log Q_{T_D^{\dagger(\phi_D^\dagger)}}(C|B, F^{(\theta)}(I))], \end{aligned} \quad (11)$$

where \bar{F} and \bar{T}_D indicate that the parameters are fixed during training. Since these additional N classifiers are domain-specific, there is a high likelihood that they can prevent F_θ from learning domain invariant features, which is against the goal of our work. But at the same time, the inclusion of $\{T_D^\dagger\}$ can help in overcoming the instability introduced by T'_D . Hence, an effective strategy for training these domain specific classifiers is of crucial importance. We initially freeze θ and train each of the classifiers $\{T_D^\dagger\}$ by using data from the D -th domain. This step will aid $\{T_D^\dagger\}$ to learn only domain invariant features. In the next step, we fix all the N parameters ϕ_D^\dagger and fine tune θ so that a sample I_D from the D -th domain is classified accurately by all $\{T_D^\dagger\}_{D \neq d}$.

The final loss function that we use to train the system is:

$$\begin{aligned} \min_{(\theta, \phi, \beta, \{\phi_D^\dagger\})} \max_{(\psi_{img}, \{\phi_D^\dagger\}, \psi_{ins})} L(\theta, \beta, \phi, \psi_{img}, \psi_{ins}, \{\phi_D^\dagger\}, \{\phi_D^\dagger\}) \\ = L_{cls}(\theta, \phi) + L_{reg}(\theta, \beta) + \alpha_1 L_{dadv}(\theta, \psi_{img}) + \\ \alpha_2 L_{dins}(\theta, \psi_{ins}) + \alpha_3 L_{cst}(\theta, \beta) + \alpha_4 L_{erc}(\theta, \{\phi_D^\dagger\}) \\ + \alpha_5 (L_{cel}(\theta, \{\phi_D^\dagger\})) \end{aligned} \quad (12)$$

where α_5 is the regularisation constant associated with the additional N domain specific classifiers $\{T_D^\dagger\}$. The complete training procedure is described in Algorithm 1, where we optimise the main detector to achieve domain invariant bounding box prediction performance; which is further used for achieving class-conditional invariance.

Algorithm 1: Training strategy for domain generalised object detection.

Input: $\{X_D\}_{D=1}^N$, N domain training datasets

Input: $\alpha_1, \alpha_2, \alpha_3, \alpha_4, \alpha_5$

Output: $F, B, T, D, D_{ins}, \{T_D\}_{D=1}^N, \{T'_D\}_{D=1}^N$

while $iter \leq MAX_EPOCHS$ **do**

 Sample data from each training dataset respectively;

 Update $\theta, \beta, \phi, \psi$ by optimising first five terms of Eq. (12);

for i **in** $1:N$ **do**

 Sample data from the D -th dataset X_D ;

 Update $\{\phi_D^\dagger\}_{D=1}^N$ by optimising the seventh term of Eq. (12);

 Update $\theta, \{\phi_D^\dagger\}_{D=1}^N$ by optimising the sixth term of Eq. (12);

 Sample data from datasets $\{X_j\}_{j=1, j \neq D}^K$;

 Update θ by optimising the seventh term of Eq. (12);

end

end

5 Experimental Validation

Datasets: We demonstrate the generalisation ability of our approach on the following four popular multi-source object detection datasets.

GWHD [25]: The aim of this dataset is to accurately detect the wheat heads from optical images captured via a wide variety of platforms, camera settings, view points and growth stages. It consists a total of 6000 images (resolution: 1024×1024 pixels) acquired across 47 different sessions; with each being restricted to a single domain/farm. The training set has 18 domains with a total of 2943 images while the validation set contains samples captured across 8 different

sessions with 1424 images and the test set has data from 21 different sessions with a total of 1434 images. Here we assume a unique domain label for each of the sessions. A few of the domains are shown in Fig. 1 illustrating the high level of domain shift across acquisition locations.

Cityscapes, Foggy Cityscapes, Rainy Cityscapes: Cityscapes [23] deals with the semantic understanding of urban street scenes. It has a total of 2975 training (from 18 cities) and 500 validation images (from 3 cities). Unlike the existing unsupervised DA based approaches [11], we train our model by using the city information as domain label and test on the Foggy Cityscapes [68] images where the fog is synthetically created using a standard fog image formation model [69] with an airlight coefficient of 0.02. Similarly, 36 different patterns of rain was introduced in 295 images of cityscapes to create rainy cityscapes dataset [70]. In order to conduct a fair comparison, we resize the original images to 600×1200 pixel resolution. Unlike the previous DA approaches, we do not use foggy/rainy images during training and also this is the first time that the Cityscapes dataset is employed in a DG setting.

BDD100k [24]: This dataset has 100K diverse video clips where each clip is of 40 seconds. The annotations are collected on six different scene types, six different weather conditions, three distinct times of the day. Unlike [68, 70], the fog and rain in the images of BDD100k is real. The train, validation, and test splits has 70K, 10K, 20K images, respectively. In our experiments, we use only train and validation splits of this dataset due to the lack of test set annotations.

Sim10k [22]: This data is generated by capturing the snapshots of Grand Theft Auto V (GTA-V) game. There is no official train and validation splits available for this dataset and hence we randomly split it into 8K images as training set and the rest as validation split. Four different weather types will appear in this dataset. We use this dataset in conjunction with cityscapes and bdd100k to extract domain invariant features corresponding to 'car' object as that is the only one which is common across all the dataset.

Network Architecture: We use Faster R-CNN as detector, with a ResNet50-FPN backbone network initialised with pre-trained ImageNet weights for GWHD and pretrained COCO weights for rest of the datasets. The feature extractor $F^{(\theta)}$ is the backbone, region proposal network and ROI pooling layer of the Faster R-CNN network. $R^{(\beta)}$ is the bounding box regressor and $T^{(\phi)}$ is to the instance level classifier components of the Faster R-CNN. The output of the backbone network is fed as input to domain adversarial network ($S^{(\psi)}$) while the output of ROI Pooling layer of the Faster R-CNN detector is fed as an input to instance level domain classifier ($S_{ins}^{(\psi)}$), $2N$ domain specific classifiers (T'_D and T_D^\dagger). All terms in the loss function described in Eq. (12) correspond to either a domain or object classifier. We use cross-entropy to train each of these classifier modules.

Training details: For all the experiments, the architecture presented in Fig. 2 was used. From empirical observations, the optimal values of the regularisation constants were found to be $\alpha_1 = 1$, $\alpha_2 = 0.1$, $\alpha_3 = 1$, $\alpha_4 = 0.001$, and $\alpha_5 = 0.05$. More details about the choice of regularisation constants can be found in supplementary material. We used early stopping with a patience of 10 epochs. AdamW (weight decay = 0.0005, learning rate = 0.001, batchsize=2) has been used as optimiser while training with GWHD and Stochastic Gradient Descent (SGD) (weight decay = 0.0005, momentum=0.9, learning rate= 2×10^{-3} , batchsize=2) has been used for other datasets (Cityscapes, BDD100K, Sim10K).

Software: The experiments were implemented using the PyTorch deep learning framework and Torchvision Faster R-CNN library.

Hardware: The experiments have been conducted on a NVIDIA Titan X GPU with 12GB of memory. Each epoch, including validation, lasted approximately 20 minutes.

Metrics: Following [25], we use weighted average domain accuracy (WADA) to report the performance of our approach on the OOD test set of GWHD. For rest of the datasets, we use mean average precision (mAP). In addition to reporting mAP as in [11], we also define and report a weighted mean AP (WmAP) as the average AP over the seven classes weighted by the number of instances in each class. This is a better metric because of the class imbalance in the dataset, which we observed causes the mean mAP to vary significantly between runs due to random noise in performance on the few classes which have only a handful of samples (e.g. 'Motorcycle').

Comparative Approaches: In this paper, our aim is to show that the proposed class-conditional invariance and bounding box invariance components should improve the generalisation ability of the main detector. Our baseline is Faster R-CNN. We re-implement the adversarial loss and consistency regulariser [11] using the [71] (MIT License) repository, and use them in for DG in the DA2018 setting. We also re-implement the entropy based classifier loss [21] for object detection, and add it to the network together with the new cross-entropy loss to demonstrate the influence of the class-conditional invariance component in the DG2020 setting. Finally, we bring all the components together and show how each of these individual components contribute to the overall generalisation ability of the detector. (For details of different losses included, see Table 1.)

Table 1: Results for the GWHD 2021 dataset. The symbol ‘+’ indicates inclusion of loss component while ‘-’ indicates exclusion of loss component.

	WADA	L_{cls}	L_{reg}	L_{dadv}	L_{dins}	L_{cst}	L_{erc}	L_{cel}
Faster R-CNN	53.73	+	+	-	-	-	-	-
DA2018	54.48	+	+	+	+	+	-	-
DG2020	53.65	+	+	+	-	-	+	+
Ours	54.92	+	+	+	+	+	+	+

Table 2: Results for the Foggy and Rainy Cityscapes datasets.

	Person	Rider	Car	Truck	Bus	Mcycle	Bicycle	mean mAP	WmAP
CityScapes Foggy									
Faster R-CNN	41.00	54.94	77.81	23.08	60.00	0	51.95	44.11	61.97
DA2018	46.41	56.48	79.71	23.07	50.00	0	53.35	44.14	64.34
DG2020	41.82	57.41	81.07	23.00	60.00	0	51.05	44.90	63.99
Ours	43.47	60.86	82.88	15.38	60.00	0	52.48	45.01	65.43
CityScapes Rainy									
Faster R-CNN	43.98	61.52	72.52	20.24	61.81	8.73	51.37	35.57	60.27
DA2018	43.18	59.83	73.29	18.25	63.43	1.59	49.62	34.35	60.02
DG2020	43.43	57.40	73.64	21.03	64.12	9.13	49.02	35.30	60.18
Ours	44.63	60.84	76.42	20.63	66.44	5.16	48.43	35.83	61.98

5.1 Quantitative Analysis

Table 1 shows the quantitative analysis for the official out-of-distribution (OOD) test split of GWHD. It can be seen that our approach outperforms the baseline Faster R-CNN used in WildS benchmark [19] as well as the competitive approaches [11, 21]. This signifies the need for the additional constraints which regularises the detector so as to equalise the conditional distributions of class-labels and bounding box detector across the domains.

While adapting Cityscapes to Foggy/Rainy Cityscapes for DG, we have purposefully followed the practices from DA. As domain shift for object detection was previously only addressed in the DA setting, we find it valuable to compare the approaches while highlighting their differences. More specifically, we chose to also study the shift from clear images (source) to foggy/rainy images (target). To realise a multi-source scenario, and learn features robust under domain shift, we include the information about the originating city during training, in contrast to DA methods which require access to the target domain images during training.

Table 2 reports the performance of our approach on the refined validation set of *Foggy Cityscapes* [68] and *Rainy Cityscapes* [70], respectively. The improved average performance of the proposed approach over baseline and existing approaches signifies the need for eliminating the covariate shift assumption to achieve a better generalisation for the detection task on the unseen target data. It can be seen that our approach has the best performance in majority of the classes from both the scenarios (foggy/rainy). However, due to the low confidence scores associated with detection of motorcycle object in fog, we see zero mean average precision for all the approaches including ours.

Table 3: Generalisation performance of the proposed approach across: Sim10K (S), Cityscapes (C) and BDD100K (B). The left and right sides of \rightarrow indicate the source and target datasets, respectively.

	(S, C) \rightarrow B	(S, B) \rightarrow C	(B, C) \rightarrow S
Faster R-CNN	50.52	71.43	61.84
DA2018 [11]	35.76	70.02	54.30
DG2020 [21]	38.07	71.27	59.50
Ours	52.02	71.78	62.50

In Table 3, we demonstrate the generalisation ability of our proposed approach on completely unseen dataset during testing. All the three datasets used here have a different image capture mechanism. In each experiment we used two of the datasets as source domains and the third one as an unseen target domain. In all the three scenarios, we observe that our approach has a better performance over [11, 21], which highlights the need for addressing both the concept and covariate shifts rather than covariate shift alone across domains.

5.2 Qualitative analysis

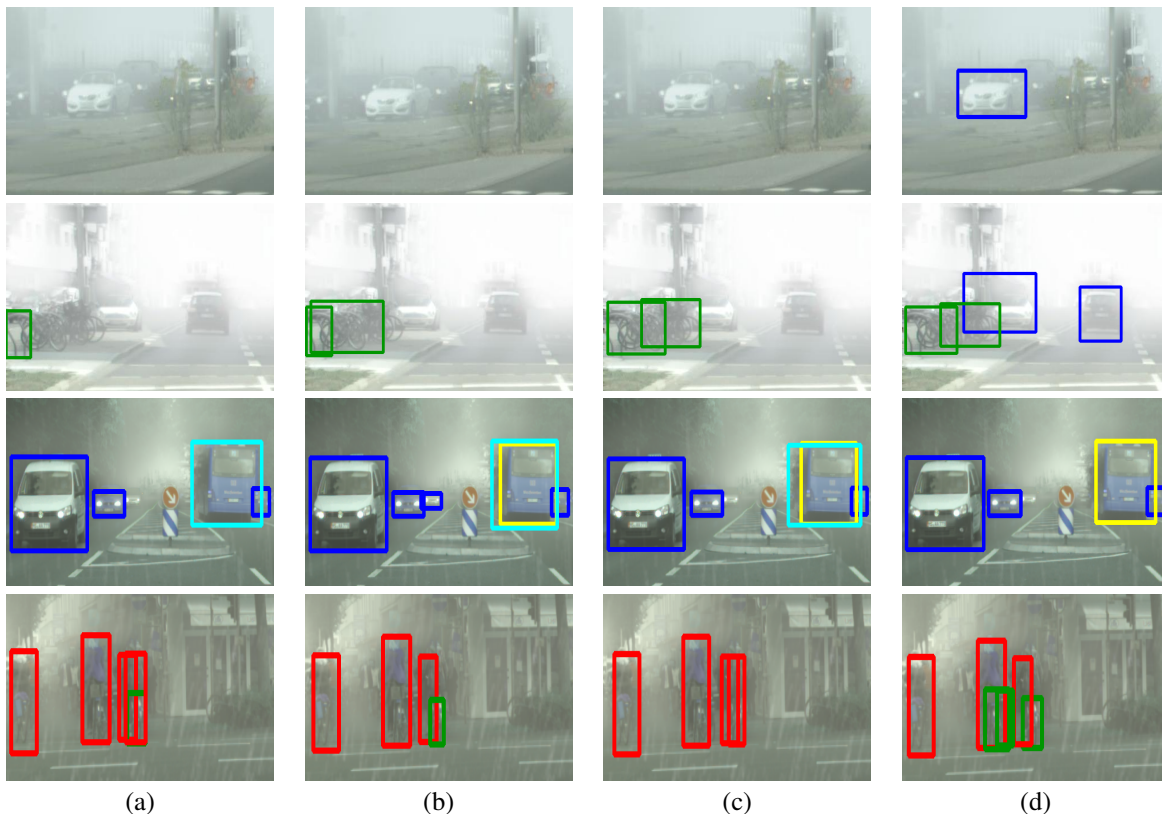


Figure 3: Qualitative Results for Cityscapes. Outputs of: (a) Faster R-CNN, (b) Chen *et al.* [11], (c) Zhao *et al.* [21], and (d) Proposed approach. (Readers are requested to zoom in to visualise the pictures.). Colour codes: Person ■, Rider ■, Car ■, Truck ■, Bus ■, Motorcycle ■, Bicycle ■.



Figure 4: Qualitative Analysis for GWHD. Color codes: Ground truth ■, Predictions ■.

Fig. 3 presents the qualitative analysis of the proposed approach against the competitive techniques (Chen *et al.* [11] (in a DG setting), Zhao *et al.* [21]) as well as the Faster R-CNN. The first two rows corresponds to Foggy-Cityscapes while the third and fourth rows shows the detections on Rainy-Cityscapes. In the first row of Fig. 3, it can be seen that the Car on the left of the road has been very well detected by our approach in spite of the dense fog being present in the scene while the state-of-the-art approaches fail to detect. Similarly, our approach robustly detects the Car in the left lane (second row Fig. 3 (d)). In the third row, the bus on the right hand side of the image is correctly detected by our approach where as the baseline or state-of-the-art approaches either incorrectly detects the bus or multiple labels are assigned to that specific object. It has to be noted that the car in the dense fog on the left side of the image is correctly detected by [11]. However, the cost of incorrectly classifying a larger size object is higher than missing a smaller size object. The bicycles in the last row of Fig. 3 are detected well by using our proposed approach over the existing techniques. We are able to accurately localise the objects in-spite of the dense fog/rain present in the scene. Note that we do not include foggy or rainy images in the training set. This emphasise the need and importance of

imposing class-conditional and bounding box invariance across all source domains to enable robust detection on the unseen target data.

Fig. 4 shows the result of wheat head detection by using our proposed approach. It can be seen that our detection is able to localise the wheat heads accurately in spite of the wide visual diversity of the wheat heads and illumination conditions.

5.3 Failure Cases



Figure 5: Failure cases in Cityscapes. (a) and (b): Multiple labels to a single object, (c) and (d): Missed detections. (Readers are requested to zoom in to visualise the pictures.)

Even though we have better detection accuracy when compared to state-of-the-art there are few failure cases on which we either do incorrect detection or miss recognising the object. Figs. 5 (a) and (b) shows an example from Cityscapes dataset where multiple labels are assigned to the same object. This incorrect assignment might be because of the similarity in the frontal appearance of Bus, Train and Car objects. Figs. 5 (c) and (d) has couple of examples where our model missed the detection. It can be seen that the pedestrians on front of the left side of the road are localised accurately but the ones in the back are missed. This might be due to the fact that our approach does not have any explicit constraint which can assist the detector to localise the occluded objects. Also, our detector misses to detect the truck in Fig. 5 (d) and this might be either due to the fog or the texture on the back of truck is not discriminative enough for the detector to localise it.



Figure 6: Failure case analysis for GWHD. First row: False detections. Second row: Missed detection due to occlusion. Third row: Missed detection due to blur. Colour codes: Predictions ■, Ground Truth ■.

We present a few instances of false detection due to shadows and bright sun light in the first row of Fig. 6. The probable reason behind this false detection is due to some of the wheat heads which appear in the same colour as of bright

sun light and also the shape of few shadows appear as wheat heads. As a future work, we plan to incorporate a few architectural advancements like [72] to suppress this false detection. The second and third row shows the missed wheat head cases due to occlusions and motion/optical blurs, respectively. We intend to model the occlusions by masking the wheat heads partially and use a few sharpening approaches as pre-processing steps to improve the wheat head detection accuracy. These failure cases will have significant impact on WADA and hence appropriate pre-processing techniques or novel architectural advancements will improve the overall performance of the detector. Please refer supplementary material for some more examples on failure cases.

6 Conclusion

We have proposed an approach for domain generalisation in the context of object detection, which can be applied to parametric feature extractor based models including but not limited to Faster R-CNN. The method has been validated by showing performance improvements when used with Faster R-CNN, on two standard datasets. Unlike the existing domain generalisation approaches for classification, the method introduced an additional consistency regularisation term to enable the detector to perform consistently across domains.

Even though the proposed method has the ability to equalise the joint probability distributions across multiple domains, we do not have any explicit constraints to eliminate the bias originating from a specific domain. An interesting future direction for generalised object detection would be to propose novel architectures to eliminate the domain specific bias completely.

The datasets used here were selected to be relevant to practical domain generalisation, each having a relatively small number of domains and many images per domain. Future experimental and theoretical work could explore the effect of this ratio. We hypothesise that the utility of the method will diminish as the number of images per domain decreases, and in the limiting case of one image per domain, a standard loss function should have the same behaviour as the new method's.

While Faster R-CNN is the current paradigm case of parametric feature extractor based models, many other current detection architectures are members of this class. For example, the backbone layers of YOLO [1] or EfficientDet [2] may be viewed as feature extractors, and separated from the upper layers of detection. Future work could test experimentally how the method improves these other models.

References

- [1] Glenn Jocher, Alex Stoken, Jirka Borovec, NanoCode012, ChristopherSTAN, Liu Changyu, Laughing, tkianai, Adam Hogan, lorenzomamma, yxNONG, AlexWang1900, Laurentiu Diaconu, Marc, wanghaoyang0106, ml5ah, Doug, Francisco Ingham, Frederik, Guilhen, Hatovix, Jake Poznanski, Jiacong Fang, Lijun Yu, changyu98, Mingyu Wang, Naman Gupta, Osama Akhtar, PetrDvoracek, and Prashant Rai. ultralytics/yolov5: v3.1 - Bug Fixes and Performance Improvements, October 2020.
- [2] Mingxing Tan, Ruoming Pang, and Quoc V Le. Efficientdet: Scalable and efficient object detection. In *Proceedings of the IEEE/CVF Conference on Computer Vision and Pattern Recognition*, pages 10781–10790, 2020.
- [3] Wei Liu, Dragomir Anguelov, Dumitru Erhan, Christian Szegedy, Scott Reed, Cheng-Yang Fu, and Alexander C Berg. SSD: Single shot multibox detector. In *European Conference on Computer Vision*, pages 21–37. Springer, 2016.
- [4] Shaoqing Ren, Kaiming He, Ross Girshick, and Jian Sun. Faster R-CNN: Towards real-time object detection with region proposal networks. *Advances in neural information processing systems*, 28:91–99, 2015.
- [5] Tsung-Yi Lin, Piotr Dollár, Ross Girshick, Kaiming He, Bharath Hariharan, and Serge Belongie. Feature pyramid networks for object detection. In *Proceedings of the IEEE Conference on Computer Vision and Pattern Recognition*, pages 2117–2125, 2017.
- [6] Jifeng Dai, Yi Li, Kaiming He, and Jian Sun. R-FCN: Object detection via region-based fully convolutional networks. In D. Lee, M. Sugiyama, U. Luxburg, I. Guyon, and R. Garnett, editors, *Advances in Neural Information Processing Systems*, volume 29. Curran Associates, Inc., 2016.
- [7] Mark Everingham, Luc Van Gool, Christopher KI Williams, John Winn, and Andrew Zisserman. The Pascal visual object classes (VOC) challenge. *International Journal of Computer Vision*, 88(2):303–338, 2010.
- [8] Tsung-Yi Lin, Michael Maire, Serge Belongie, James Hays, Pietro Perona, Deva Ramanan, Piotr Dollár, and C Lawrence Zitnick. Microsoft COCO: Common objects in context. In *European Conference on Computer Vision*, pages 740–755. Springer, 2014.

- [9] Benjamin Recht, Rebecca Roelofs, Ludwig Schmidt, and Vaishaal Shankar. Do imagenet classifiers generalize to imagenet? In *International Conference on Machine Learning*, pages 5389–5400. PMLR, 2019.
- [10] Dan Hendrycks and Thomas Dietterich. Benchmarking neural network robustness to common corruptions and perturbations. *arXiv preprint arXiv:1903.12261*, 2019.
- [11] Yuhua Chen, Wen Li, Christos Sakaridis, Dengxin Dai, and Luc Van Gool. Domain adaptive Faster R-CNN for object detection in the wild. In *Proceedings of the IEEE Conference on Computer Vision and Pattern Recognition*, pages 3339–3348, 2018.
- [12] Minjie Cai, Minyi Luo, Xionghu Zhong, and Hao Chen. Uncertainty-aware model adaptation for unsupervised cross-domain object detection. *arXiv preprint arXiv:2108.12612*, 2021.
- [13] Kuniaki Saito, Yoshitaka Ushiku, Tatsuya Harada, and Kate Saenko. Strong-weak distribution alignment for adaptive object detection. In *Proceedings of the IEEE/CVF Conference on Computer Vision and Pattern Recognition*, pages 6956–6965, 2019.
- [14] Chang-Dong Xu, Xing-Ran Zhao, Xin Jin, and Xiu-Shen Wei. Exploring categorical regularization for domain adaptive object detection. In *Proceedings of the IEEE/CVF Conference on Computer Vision and Pattern Recognition*, pages 11724–11733, 2020.
- [15] Wanyi Li, Fuyu Li, Yongkang Luo, Peng Wang, et al. Deep domain adaptive object detection: A survey. In *2020 IEEE Symposium Series on Computational Intelligence (SSCI)*, pages 1808–1813. IEEE, 2020.
- [16] Han-Kai Hsu, Chun-Han Yao, Yi-Hsuan Tsai, Wei-Chih Hung, Hung-Yu Tseng, Maneesh Singh, and Ming-Hsuan Yang. Progressive domain adaptation for object detection. In *Proceedings of the IEEE/CVF Winter Conference on Applications of Computer Vision*, pages 749–757, 2020.
- [17] Da Li, Yongxin Yang, Yi-Zhe Song, and Timothy M Hospedales. Deeper, broader and artier domain generalization. In *Proceedings of the IEEE International Conference on Computer Vision*, pages 5542–5550, 2017.
- [18] Kaiyang Zhou, Ziwei Liu, Yu Qiao, Tao Xiang, and Chen Change Loy. Domain generalization: A survey. *arXiv preprint arXiv:2103.02503*, 2021.
- [19] Pang Wei Koh, Shiori Sagawa, Sang Michael Xie, Marvin Zhang, Akshay Balsubramani, Weihua Hu, Michihiro Yasunaga, Richard Lanus Phillips, Irena Gao, Tony Lee, et al. Wilds: A benchmark of in-the-wild distribution shifts. In *International Conference on Machine Learning*, pages 5637–5664. PMLR, 2021.
- [20] Hong Liu, Pinhao Song, and Runwei Ding. Towards domain generalization in underwater object detection. In *2020 IEEE International Conference on Image Processing (ICIP)*, pages 1971–1975. IEEE, 2020.
- [21] Shanshan Zhao, Mingming Gong, Tongliang Liu, Huan Fu, and Dacheng Tao. Domain generalization via entropy regularization. *Advances in Neural Information Processing Systems*, 33, 2020.
- [22] Matthew Johnson-Roberson, Charles Barto, Rounak Mehta, Sharath Nittur Sridhar, Karl Rosaen, and Ram Vasudevan. Driving in the matrix: Can virtual worlds replace human-generated annotations for real world tasks? In *2017 IEEE International Conference on Robotics and Automation (ICRA)*, pages 746–753. IEEE, 2017.
- [23] Marius Cordts, Mohamed Omran, Sebastian Ramos, Timo Rehfeld, Markus Enzweiler, Rodrigo Benenson, Uwe Franke, Stefan Roth, and Bernt Schiele. The Cityscapes dataset for semantic urban scene understanding. In *Proceedings of the IEEE Conference on Computer Vision and Pattern Recognition*, pages 3213–3223, 2016.
- [24] Fisher Yu, Haofeng Chen, Xin Wang, Wenqi Xian, Yingying Chen, Fangchen Liu, Vashisht Madhavan, and Trevor Darrell. Bdd100k: A diverse driving dataset for heterogeneous multitask learning. In *Proceedings of the IEEE/CVF conference on computer vision and pattern recognition*, pages 2636–2645, 2020.
- [25] Etienne David, Mario Serouart, Daniel Smith, Simon Madec, Kaaviya Velumani, Shouyang Liu, Xu Wang, Francisco Pinto, Shahameh Shafiee, Izzat SA Tahir, et al. Global wheat head detection 2021: an improved dataset for benchmarking wheat head detection methods. *Plant Phenomics*, 2021, 2021.
- [26] Chen Fang, Ye Xu, and Daniel N Rockmore. Unbiased metric learning: On the utilization of multiple datasets and web images for softening bias. In *Proceedings of the IEEE International Conference on Computer Vision*, pages 1657–1664, 2013.
- [27] Kate Saenko, Brian Kulis, Mario Fritz, and Trevor Darrell. Adapting visual category models to new domains. In *European Conference on Computer Vision*, pages 213–226. Springer, 2010.
- [28] Antonio Torralba and Alexei A Efros. Unbiased look at dataset bias. In *CVPR 2011*, pages 1521–1528. IEEE, 2011.
- [29] Navneet Dalal and Bill Triggs. Histograms of oriented gradients for human detection. In *2005 IEEE Computer Society Conference on Computer Vision and Pattern Recognition (CVPR'05)*, volume 1, pages 886–893. Ieee, 2005.

- [30] Pedro F Felzenszwalb, Ross B Girshick, David McAllester, and Deva Ramanan. Object detection with discriminatively trained part-based models. *IEEE Transactions on Pattern Analysis and Machine Intelligence*, 32(9):1627–1645, 2009.
- [31] Paul Viola and Michael Jones. Rapid object detection using a boosted cascade of simple features. In *Proceedings of the 2001 IEEE Computer Society Conference on Computer Vision and Pattern Recognition. CVPR 2001*, volume 1, pages I–I. Ieee, 2001.
- [32] Yann LeCun, Léon Bottou, Yoshua Bengio, and Patrick Haffner. Gradient-based learning applied to document recognition. *Proceedings of the IEEE*, 86(11):2278–2324, 1998.
- [33] Alex Krizhevsky, Ilya Sutskever, and Geoffrey E Hinton. Imagenet classification with deep convolutional neural networks. *Advances in neural information processing systems*, 25:1097–1105, 2012.
- [34] Joseph Redmon, Santosh Divvala, Ross Girshick, and Ali Farhadi. You only look once: Unified, real-time object detection. In *Proceedings of the IEEE Conference on Computer Vision and Pattern Recognition*, pages 779–788, 2016.
- [35] Ross Girshick, Jeff Donahue, Trevor Darrell, and Jitendra Malik. Rich feature hierarchies for accurate object detection and semantic segmentation. In *Proceedings of the IEEE Conference on Computer Vision and Pattern Recognition*, pages 580–587, 2014.
- [36] Ross Girshick. Fast R-CNN. In *Proceedings of the IEEE International Conference on Computer Vision*, pages 1440–1448, 2015.
- [37] Ya Li, Xinmei Tian, Mingming Gong, Yajing Liu, Tongliang Liu, Kun Zhang, and Dacheng Tao. Deep domain generalization via conditional invariant adversarial networks. In *Proceedings of the European Conference on Computer Vision (ECCV)*, pages 624–639, 2018.
- [38] Bernhard Schölkopf, Dominik Janzing, Jonas Peters, Eleni Sgouritsa, Kun Zhang, and Joris Mooij. On causal and anticausal learning. *arXiv preprint arXiv:1206.6471*, 2012.
- [39] Dominik Janzing and Bernhard Schölkopf. Causal inference using the algorithmic markov condition. *IEEE Transactions on Information Theory*, 56(10):5168–5194, 2010.
- [40] Vishwanath A Sindagi, Poojan Oza, Rajeev Yasarla, and Vishal M Patel. Prior-based domain adaptive object detection for hazy and rainy conditions. In *European Conference on Computer Vision*, pages 763–780. Springer, 2020.
- [41] Zhenwei He and Lei Zhang. Multi-adversarial Faster R-CNN for unrestricted object detection. In *Proceedings of the IEEE/CVF International Conference on Computer Vision*, pages 6668–6677, 2019.
- [42] Xinge Zhu, Jiangmiao Pang, Ceyuan Yang, Jianping Shi, and Dahua Lin. Adapting object detectors via selective cross-domain alignment. In *Proceedings of the IEEE/CVF Conference on Computer Vision and Pattern Recognition*, pages 687–696, 2019.
- [43] Aming Wu, Yahong Han, Linchao Zhu, and Yi Yang. Instance-invariant domain adaptive object detection via progressive disentanglement. *IEEE Transactions on Pattern Analysis and Machine Intelligence*, 2021.
- [44] Adrian Lopez Rodriguez and Krystian Mikolajczyk. Domain adaptation for object detection via style consistency. In *Proceedings BMVC*, 2019.
- [45] Rui Gong, Wen Li, Yuhua Chen, and Luc Van Gool. Dlow: Domain flow for adaptation and generalization. In *Proceedings of the IEEE/CVF Conference on Computer Vision and Pattern Recognition*, pages 2477–2486, 2019.
- [46] Mehran Khodabandeh, Arash Vahdat, Mani Ranjbar, and William G Macready. A robust learning approach to domain adaptive object detection. In *Proceedings of the IEEE/CVF International Conference on Computer Vision*, pages 480–490, 2019.
- [47] Aruni RoyChowdhury, Prithvijit Chakrabarty, Ashish Singh, SouYoung Jin, Huaizu Jiang, Liangliang Cao, and Erik Learned-Miller. Automatic adaptation of object detectors to new domains using self-training. In *Proceedings of the IEEE/CVF Conference on Computer Vision and Pattern Recognition*, pages 780–790, 2019.
- [48] Xingxu Yao, Sicheng Zhao, Pengfei Xu, and Jufeng Yang. Multi-source domain adaptation for object detection. In *Proceedings of the IEEE/CVF International Conference on Computer Vision*, pages 3273–3282, 2021.
- [49] Gilles Blanchard, Gyemin Lee, and Clayton Scott. Generalizing from several related classification tasks to a new unlabeled sample. *Advances in neural information processing systems*, 24:2178–2186, 2011.
- [50] Krikamol Muandet, David Balduzzi, and Bernhard Schölkopf. Domain generalization via invariant feature representation. In *International Conference on Machine Learning*, pages 10–18. PMLR, 2013.

- [51] Muhammad Ghifary, W Bastiaan Kleijn, Mengjie Zhang, and David Balduzzi. Domain generalization for object recognition with multi-task autoencoders. In *Proceedings of the IEEE International Conference on Vision*, pages 2551–2559, 2015.
- [52] Aditya Khosla, Tinghui Zhou, Tomasz Malisiewicz, Alexei A Efros, and Antonio Torralba. Undoing the damage of dataset bias. In *European Conference on Computer Vision*, pages 158–171. Springer, 2012.
- [53] Zheng Xu, Wen Li, Li Niu, and Dong Xu. Exploiting low-rank structure from latent domains for domain generalization. In *European Conference on Computer Vision*, pages 628–643. Springer, 2014.
- [54] Da Li, Yongxin Yang, Yi-Zhe Song, and Timothy M Hospedales. Learning to generalize: Meta-learning for domain generalization. In *Thirty-Second AAAI Conference on Artificial Intelligence*, 2018.
- [55] Shiv Shankar, Vihari Piratla, Soumen Chakrabarti, Siddhartha Chaudhuri, Preethi Jyothi, and Sunita Sarawagi. Generalizing across domains via cross-gradient training. In *ICLR*, 2018.
- [56] Da Li, Jianshu Zhang, Yongxin Yang, Cong Liu, Yi-Zhe Song, and Timothy M Hospedales. Episodic training for domain generalization. In *Proceedings of the IEEE/CVF International Conference on Computer Vision*, pages 1446–1455, 2019.
- [57] Josh Tobin, Rachel Fong, Alex Ray, Jonas Schneider, Wojciech Zaremba, and Pieter Abbeel. Domain randomization for transferring deep neural networks from simulation to the real world. In *2017 IEEE/RSJ International Conference on Intelligent Robots and Systems (IROS)*, pages 23–30. IEEE, 2017.
- [58] Xiangyu Yue, Yang Zhang, Sicheng Zhao, Alberto Sangiovanni-Vincentelli, Kurt Keutzer, and Boqing Gong. Domain randomization and pyramid consistency: Simulation-to-real generalization without accessing target domain data. In *Proceedings of the IEEE/CVF International Conference on Computer Vision*, pages 2100–2110, 2019.
- [59] Shoubo Hu, Kun Zhang, Zhitang Chen, and Laiwan Chan. Domain generalization via multidomain discriminant analysis. In *Uncertainty in Artificial Intelligence*, pages 292–302. PMLR, 2020.
- [60] Haoliang Li, Sinno Jialin Pan, Shiqi Wang, and Alex C Kot. Domain generalization with adversarial feature learning. In *Proceedings of the IEEE Conference on Computer Vision and Pattern Recognition*, pages 5400–5409, 2018.
- [61] Rawal Khirodkar, Donghyun Yoo, and Kris Kitani. Domain randomization for scene-specific car detection and pose estimation. In *2019 IEEE Winter Conference on Applications of Computer Vision (WACV)*, pages 1932–1940. IEEE, 2019.
- [62] Hong Liu, Pinhao Song, and Runwei Ding. WQT and DG-YOLO: Towards domain generalization in underwater object detection. *arXiv preprint arXiv:2004.06333*, 2020.
- [63] Martin Arjovsky, Léon Bottou, Ishaan Gulrajani, and David Lopez-Paz. Invariant risk minimization. *arXiv preprint arXiv:1907.02893*, 2019.
- [64] Elan Rosenfeld, Pradeep Ravikumar, and Andrej Risteski. The risks of invariant risk minimization. *arXiv preprint arXiv:2010.05761*, 2020.
- [65] Toshihiko Matsuura and Tatsuya Harada. Domain generalization using a mixture of multiple latent domains. In *Proceedings of the AAAI Conference on Artificial Intelligence*, volume 34, pages 11749–11756, 2020.
- [66] Ian J Goodfellow, Jean Pouget-Abadie, Mehdi Mirza, Bing Xu, David Warde-Farley, Sherjil Ozair, Aaron Courville, and Yoshua Bengio. Generative adversarial networks. *arXiv preprint arXiv:1406.2661*, 2014.
- [67] Mingming Gong, Yanwu Xu, Chunyuan Li, Kun Zhang, and Kayhan Batmanghelich. Twin auxiliary classifiers GAN. *Advances in neural information processing systems*, 32:1328, 2019.
- [68] Christos Sakaridis, Dengxin Dai, and Luc Van Gool. Semantic foggy scene understanding with synthetic data. *International Journal of Computer Vision*, 126(9):973–992, Sep 2018.
- [69] William Edgar Knowles Middleton. Vision through the atmosphere. In *Geophysik II/Geophysics II*, pages 254–287. Springer, 1957.
- [70] Xiaowei Hu, Chi-Wing Fu, Lei Zhu, and Pheng-Ann Heng. Depth-attentional features for single-image rain removal. In *Proceedings of the IEEE/CVF Conference on Computer Vision and Pattern Recognition (CVPR)*, June 2019.
- [71] sumiya-NJU Jianwei Yang. <https://github.com/tiancity-NJU/da-faster-rcnn-PyTorch>, 2008. [Online; accessed 19-July-2008].
- [72] Chengxin Liu, Kewei Wang, Hao Lu, and Zhiguo Cao. Dynamic color transform for wheat head detection. In *Proceedings of the IEEE/CVF International Conference on Computer Vision*, pages 1278–1283, 2021.

[73] Dominik Maria Endres and Johannes E Schindelin. A new metric for probability distributions. *IEEE Transactions on Information theory*, 49(7):1858–1860, 2003.

A Theoretical Proof

Theorem 1: Assuming all the object classes are equally likely, maximising $H_D(C^I|B^I, F^{(\theta)}(I))$ is equivalent to minimising the Jensen-Shannon divergence between the conditional distributions $P_D(B^I, F^{(\theta)}(I)|C = j)_{j=1}^K$. The global minimum can be achieved if and only if:

$$P_D(B^I, F^{(\theta)}(I)|C^I = i) = P_D(B^I, F^{(\theta)}(I)|C^I = j), \quad \forall i, j \in \{1, \dots, K\}. \quad (13)$$

Even though this assumption can fail under a class imbalance scenario, balance can still be enforced through batch based biased sampling.

Proof: In this proof, we use the derivation provided in the supplementary material of [21] and adopt it for object detection problem by additionally including the bounding box predictor B within our mathematical framework. Also, we will be using the following definitions on information gain, Kullback-Leibler divergence and Jensen-Shannon divergence in our proof.

The information gain G between any two random variables L and M is usually defined as:

$$G(L, M) = H(L) - H(L|M), \quad (14)$$

where H denotes the entropy associated with a random variable. Let $P_D(L)$ and $P_D(M)$ be the probability distributions associated with the random variables L and M , respectively. The distance between $P_D(L)$ and $P_D(M)$ can be measured by using the Kullback-Leibler (KL) divergence and is expressed as:

$$KL(P_D(L)||P_D(M)) = \mathbb{E} \left[\log \frac{P_D(L)}{P_D(M)} \right]. \quad (15)$$

Let L be a discrete random variable which can take the values between $\{1, \dots, K\}$, then the relation between Kullback-Leibler (KL) divergence and Jensen-Shannon (JS) divergence is [73]:

$$JS(P(M|L = 1), P(M|L = 2), \dots, P(M|L = K)) = \frac{1}{K} \sum_{i=1}^K KL(P(M|L = i)||P(M)). \quad (16)$$

By using the definition in Eq. (14), the negative class conditional entropy can be expressed as

$$-H_D(C^I|B^I, F^{(\theta)}(I)) = G_D(F^{(\theta)}(I), C^I, B^I) - H_D(C^I) \quad (17)$$

The first term of Eq. (17) can be expanded as

$$\begin{aligned} G_D(F^{(\theta)}(I), C^I, B^I) &= H_D(F^{(\theta)}(I), B^I) - H_D(F^{(\theta)}(I), B^I|C^I) \\ &= \frac{1}{K} \sum_{c=1}^K \mathbb{E} \left[\log \frac{P_D(F^{(\theta)}(I), B^I|C^I = c)}{P_D(F^{(\theta)}(I), B^I)} \right] \\ &= \frac{1}{K} \sum_{c=1}^K KL(P_D(F^{(\theta)}(I), B^I|C^I = c)||P_D(F^{(\theta)}(I), B^I)). \end{aligned} \quad (18)$$

From Eqs. (17) and (18), it is clear that minimising the domain specific negative class conditional entropy $-H_D(C^I|B^I, F^{(\theta)}(I))$ is equivalent to minimising the KL-divergence between $P_D(F^{(\theta)}(I), B^I|C^I)$ and $P_D(F^{(\theta)}(I), B^I)$. By using Eq. (16), minimising the KL divergence in Eq. (18) is equivalent to minimising the following Jensen-Shannon divergence

$$JS(P_D(F^{(\theta)}(I), B^I|C^I = 1), P_D(F^{(\theta)}(I), B^I|C^I = 2), \dots, P_D(F^{(\theta)}(I), B^I|C^I = K)) \quad (19)$$

whose global minimum occurs under the following condition

$$P_D(B^I, F^{(\theta)}(I)|C^I = i) = P_D(B^I, F^{(\theta)}(I)|C^I = j), \forall i, j \in \{1, \dots, K\}. \quad (20)$$

The intuition behind Eq. (20) is that the minimisation of class conditional entropy results in domain specific instance level features which do not have the discriminative ability to assign the correct class label corresponding to the objects in the image I . As mentioned in the main paper, we realise the result in Eq. (20) by introducing the additional N domain specific classifiers. Also, following [21], we use gradient reversal layer (GRL) to aid the feature extractor lose the discriminative ability while minimising the domain specific classification loss.

B Choice of regularisation constants

In our proposed approach, there are five additional loss terms along with main detection loss and can help the main detector to achieve the class conditional and bounding box invariance across the domains. We start with the default regularisation constants as suggested by [11, 21] and vary the values around those default values. Table 4 shows the various combinations that we tried while fine tuning the hyperparameters of our model using the validation set of cityscapes. The first row indicates the performance of our approach using the default values of the regularisation constants [11]. Rows 2-5 of Table 4 shows the performance of the trained model when loss terms corresponding to bounding box invariance are enabled. It can be seen that the best performance is obtained in the third row where $(\alpha_1, \alpha_2, \alpha_3) = (1, 0.1, 1)$ which indicates that the image level domain classifier contributes more to the performance of the model than the instance level domain classifier. The primary reason behind such a behaviour is due to the fact that the domain label (city information) used majorly capture global changes rather than diversity across various instances. The sixth and seventh rows in Table 4 shows the influence of class conditional invariance in conjunction with domain discriminator as used in [21]. It can be seen that the combination $(\alpha_1, \alpha_4, \alpha_5) = (1, 0.001, 0.05)$ works the best. With these observations we use the combination $(\alpha_1, \alpha_2, \alpha_3, \alpha_4, \alpha_5) = (1, 0.1, 1, 0.001, 0.05)$ while training our proposed model and it can be seen from (8th row of Table 4) that integrating all the components can help us to improve over the individual components helping the main detector to extract generalised features for object detection.

α_1	α_2	α_3	α_4	α_5	mAP	wmAP
0.1	0.1	0.1	0	0	46.25	54.32
0.5	0.1	1	0	0	46.08	54.11
1	0.1	1	0	0	47.02	54.38
1	0.001	1	0	0	37.89	53.73
1	0.05	1	0	0	36.62	52.05
1	0	0	0.001	0.05	45.45	55.02
1	0	0	0.05	0.001	45.88	53.44
1	0.1	1	0.001	0.05	47.24	55.56
1	0.05	1	0.001	0.05	44.92	53.65
1	0.001	1	0.001	0.05	34.22	50.30
1	0.05	0.05	0.001	0.05	37.54	52.79

Table 4: Choice of regularisation constants.